Available online at www.sciencedirect.com
ScienceDirect
Biochimica et Biophysica Acta 1778 (2008) 872–879
Biochimica et Biophysica Acta
BBA
www.elsevier.com/locate/bbamem

# Secondary structure and orientation of the pore-forming toxin lysenin in a sphingomyelin-containing membrane

Monika Hereć [a,b], Mariusz Gagoś [c], Magdalena Kulma [a], Katarzyna Kwiatkowska [a], Andrzej Sobota [a,*], Wiesław I. Gruszecki [d,*]

[a] Department of Cell Biology, Nencki Institute of Experimental Biology, 02-093 Warsaw, Poland
[b] Department of Theoretical Physics, The John Paul II Catholic University of Lublin, 20-950 Lublin, Poland
[c] Department of Physics, Agricultural University, 20-033 Lublin, Poland
[d] Department of Biophysics, Institute of Physics, Maria Curie-Skłodowska University, 20-031 Lublin, Poland

Received 20 June 2007; received in revised form 29 October 2007; accepted 7 December 2007
Available online 15 December 2007

**Abstract**

Lysenin is a sphingomyelin-recognizing toxin which forms stable oligomers upon membrane binding and causes cell lysis. To get insight into the mechanism of the transition of lysenin from a soluble to a membrane-bound form, surface activity of the protein and its binding to lipid membranes were studied using tensiometric measurements, Fourier-transform infrared spectroscopy (FTIR) and FTIR-linear dichroism. The results showed cooperative adsorption of recombinant lysenin-His at the argon–water interface from the water subphase which suggested self-association of lysenin-His in solution. An assembly of premature oligomers by lysenin-His in solution was confirmed by blue native gel electrophoresis. When a monolayer composed of sphingomyelin and cholesterol was present at the interface, the rate of insertion of lysenin-His into the monolayer was considerably enhanced. Analysis of FTIR spectra of soluble lysenin-His demonstrated that the protein contained 27% β-sheet, 28% aggregated β-strands, 10% α-helix, 23% turns and loops and 12% different kinds of aggregated forms. In membrane-bound lysenin-His the total content of α-helices, turns and loops, and β-structures did not change, however, the 1636cm$^{-1}$ β-sheet band increased from 18% to 31% at the expense of the 1680cm$^{-1}$ β-sheet structure. Spectral analysis of the amide I band showed that the α-helical component was oriented with at 41° to the normal to the membrane, indicating that this protein segment could be anchored in the hydrophobic core of the membrane.


*Keywords:* Lysenin; Toxin; Sphingomyelin; Monolayer; Secondary structure determination by FTIR spectroscopy; FTIR-linear dichroism

## 1. Introduction

Lysenin is a 297-amino acid protein belonging to the group of cytolytic and bacteriostatic toxins isolated from the coelomic fluid of the earthworm *Eisenia foetida* [1,2]. The unique and the most interesting property of this toxin is its ability specifically to interact with sphingomyelin, a major plasma membrane lipid in animal cells [1–3]. Binding of lysenin to other sphingolipids, glycerophospholipids or cholesterol has not been observed [1,4]. Upon binding to sphingomyelin, lysenin forms oligomers that were first identified as SDS-resistant hexamers and visualized as hexagonal structures of 10-nm external diameter with a 3-nm pore inside [4,5]. Subsequent analysis using blue native gel electrophoresis revealed that trimer can be the functional unit of the protein associated with the membrane [5]. The lysenin's ability to oligomerize seems to be correlated with its lytic activity. After truncation of 160 N-terminal amino acids and a point mutation of the single tryptophan 20, both oligomerization and the cytolytic activity were abrogated despite unaltered sphingomyelin binding [5,6]. The lytic action of wild type lysenin relies on the formation of ion channels disturbing the ion balance in the cell, however, at higher concentrations of the protein membrane rupture takes place [5,7].

* Corresponding authors. A. Sobota is to be contacted at The Nencki Institute of Experimental Biology, Department of Cell Biology, 3 Pasteur St., 02-093 Warsaw. Tel.: +48 22 5892 234; fax: +48 22 822 5342. W.I. Gruszecki, tel.: +48 81 5376 252; fax: +48 81 537 6191.
*E-mail addresses:* a.sobota@nencki.gov.pl (A. Sobota), wieslaw.gruszecki@umcs.lublin.pl (W.I. Gruszecki).

0005-2736/$ - see front matter © 2007 Elsevier B.V. All rights reserved.
doi:10.1016/j.bbamem.2007.12.004

Although not required for sphingomyelin binding, cholesterol facilities lysenin oligomerization [1,8]. Since a single lysenin molecule binds five sphingomyelin molecules and the toxin preferentially recognizes sphingomyelin when the lipid forms clusters [9,10], the effect of cholesterol could ensue from facilitated phase separation between sphingomyelin-rich liquid-ordered domains and the liquid-disordered glycerophospholipid-rich milieu. However, recent data indicate that cholesterol affects lysenin oligomerization by fluidizing sphingomyelin-rich domains rather than via facilitating phase separation. As a result, an interaction of sphingomyelin-bound lysenin molecules is promoted facilitating the protein oligomerization [8].

Apart from model membranes, sphingomyelin and cholesterol of the plasma membrane are thought to participate in the assembly of lipid microdomains, so-called rafts. These structures are recognized to play an important role in many cellular functions, especially in signal transduction [11–13]. The engagement of sphingomyelin in raft organization and cellular signalling has sparked interest in lysenin as a tool to study sphingomyelin distribution and function in the plasma membrane. Upon interaction with sphingomyelin, lysenin transforms from a water-soluble to a membrane-embedded form in an as yet not fully understood manner. Our earlier prediction of the secondary structure of lysenin posited that more than half of the residues tend to form β structures (53%), 23% form turns and loops, and 6% form α-helix. However, determination of the secondary structure by another method revealed no helical segments in the lysenin molecule, and the transmembrane domain of the protein also remained unidentified [2].

The monomolecular lipid layer studies presented in this report allowed a direct observation of insertion of recombinant lysenin-His into model lipid membranes composed of sphingomyelin and cholesterol. Fourier-transform infrared absorption spectroscopy (FTIR) was used to determine the secondary structure of lysenin-His, free and incorporated in lipid membranes, while orientation of the membrane-bound protein was examined by polarized IR radiation. The experiments allowed investigation of the structural changes of lysenin depending on its environment, especially in the course of the binding to the membrane and pointed to an α-helix as a possible membrane-inserting fragment of the protein.

## 2. Materials and methods

### 2.1. Materials

We synthesized the gene of lysenin fused with a polyhistidine tag at the N-terminus (lysenin-His) from DNA oligos by PCR as described [5], using the nucleotide sequence of lysenin cDNA cloned by Sekizawa et al. [14]. The recombinant protein was expressed in *Escherichia coli* and purified according to [5] with modifications (E. Czuryło, in preparation). For measurements, lysenin-His was equilibrated with 60mM NaCl and 10mM Tris-buffer (pH 7.7). Bovine brain sphingomyelin and cholesterol were purchased from Sigma-Aldrich Chemicals. Lipids were stored under argon at − 80°C. Lipid stock solutions were prepared in chloroform.

### 2.2. Monomolecular layer technique measurements

Monomolecular lipid layers were formed in a Teflon trough. Water used in all experiments was double distilled and deionized. In order to remove possible organic impurities the water was distilled for a third time with $KMnO_4$. Surface pressure was monitored by a NIMA Technology tensiometer, model PS3 (Coventry, UK). Monolayer experiments were carried out at 21 ± 1°C. Experiments were performed in darkness under argon atmosphere in order to avoid oxidative degradation of lipids. Two-component monolayer of sphingomyelin and cholesterol, at the molar ratio of 1:1, were deposited at the argon–water interface from chloroform solution. The water subphase was buffered with 10mM Tris–HCl (pH 7.7). A stock solution (20μl) of lysenin-His was injected to 12ml of the subphase. Final lysenin-His concentration in the subphase after single injection was 70nM.

### 2.3. FTIR measurements

The secondary structure of lysenin-His was estimated by analyzing FTIR spectra. Attenuated total reflection infrared (ATR-FTIR) spectra of lysenin-His deposited on the ATR crystal element by partial evaporation and of lysenin-His-containing lipid membranes were recorded with a Vector 33 spectrometer (Bruker, Germany). The internal reflection element was a Ge crystal (45° cut) yielding 10 internal reflections. Typically, 30 scans were collected, Fourier-transformed and averaged for each measurement. Absorption spectra at a resolution of one data point every $4cm^{-1}$ were obtained in the region between 4000 and $400cm^{-1}$ using a clean crystal as the background. The instrument was continuously purged with argon for 40min before and during measurements. The ATR crystals were cleaned with organic solvents. All experiments were done at 21°C. A wire grid infrared polarizer KRS-5 (Pike Technologies, USA) was used in the IR linear dichroism experiments. Spectral analysis was performed with OPUS (Bruker, Germany) and Grams 32 software from Galactic Industries (USA).

### 2.4. Bilayer preparation

The ATR-FTIR investigation of the binding of lysenin-His to lipid membranes required preparation of a lipid bilayer composed of sphingomyelin and cholesterol (1:1, mol:mol) at the surface of the Ge crystal. The "attach" technique was applied to deposit the first lipid monolayer, the so-called supporting lipid layer, directly on the crystal surface [15]. The surface pressure of the monolayer attached to the Ge crystal was adjusted to 22mN/m. The second monolayer was then deposited by approaching of the crystal (with the monolayer attached) to a lipid monolayer formed previously at the surface of the buffer in the Teflon dish, inside the ATR attachment. IR absorption spectra of the lipid bilayer were collected before and after the injection of lysenin-His into the aqueous subphase. For spectroscopic measurements of pure lysenin-His, directly before the measurements the protein stock solution prepared in the $H_2O$-based buffer was 100-fold diluted with $D_2O$ and the protein was deposited onto the Ge support by evaporation under the stream of gaseous argon. Such a procedure yields removal of bulk water but retains so-called "structural water" tightly bound to protein. Short time of experiment prevents H/D exchange. Pronounced H/D exchange did not take place since a shift of the position of the amide II band of lysenin-His has not been observed.

### 2.5. Linear dichroism measurements

The FTIR technique with polarization of the IR beam provides information on the orientation of the protein secondary structure elements embedded in the lipid bilayer with the lipid acyl chains oriented perpendicular to the surface of the ATR plate.

The dichroic ratio ($R$) is defined as the ratio of integrated absorption bands or the absorbance values corresponding to the selected vibrational modes in the parallel ($A_{\|}$) and perpendicular ($A_{\perp}$) configuration [16]:

$$R = \frac{A_{\|}}{A_{\perp}} = \frac{\int A_{\|}(v)dv}{\int A_{\perp}(v)dv} \quad (1)$$

The order parameter $S$ is a space averaged function of the $\theta$ angle between the molecular director and the molecular axis with respect to the axis perpendicular to the plane of the membrane ($z$ axis). The order parameter ($S$) is defined as:

$$S = \frac{(3<\cos^2\theta> - 1)}{2} \quad (2)$$

In turn, $S$ is related to the dichroic ratio by:

$$S = \frac{E_x^2 - RE_y^2 + E_z^2}{\frac{1}{2}(3\cos^2\alpha - 1)\left(E_x^2 - RE_y^2 - 2E_z^2\right)} \quad (3)$$

where $\alpha$ is the angle between the transition dipole moment of the investigated vibration and the molecular director of the molecule [17–19]. $E_x$, $E_y$ and $E_z$ are the components of the electric field of the evanescent wave in the three directions, dependent on the angle of incidence of the IR beam (45°), refractive indices of the internal reflection Ge plate (4.0), of the supported lipid membrane (1.40), and of water (1.33) [20]. The values of $E_x^2 = 1.97$, $E_y^2 = 2.25$ and $E_z^2 = 2.08$. The nominal penetration depth of the electromagnetic field into the sample is for Ge crystals between 1.1 and 1.5μm [20].

### 2.6. Determination of orientation of the protein

According to the literature, the angle $\alpha$ between the transition dipole moment and the α-helix long axis is in the range between 29° and 40° [21]. We used a value of 39° in our calculations.

### 2.7. Secondary structure analysis

Determination of the secondary structure of lysenin-His was based on an analysis of the amide I band (between 1600 and 1700cm$^{-1}$). The band was deconvoluted with a combination of Lorentzian–Gaussian components. The relative content of particular secondary structure component was estimated by dividing the areas of individual components by the area of whole amide I band.

In the case of non-oriented samples of lysenin-His deposited on the Ge crystal, the spectrum to be analyzed was recorded with non-polarized light. For the oriented samples of the lipid-bound lysenin-His, the band fitting was done for the spectrum which was a linear combination of the absorption spectra recorded with radiation polarized parallel $A_{\parallel}$ with and perpendicular $A_{\perp}$ to the plane of incidence according to the formula of Marsh [22]:

$$A = A_{\parallel} + GA_{\perp} \quad (4)$$

where:

$$G = \left(2E_z^2 - E_x^2\right)/E_y^2 \quad (5)$$

$E_x$, $E_y$, $E_z$ are the orthogonal electric vector components of the evanescent field in the membrane.

### 2.8. Blue native gel electrophoresis and SDS-PAGE

For blue native gel electrophoresis, lysenin-His (0.2mg/ml) was equilibrated with solubilization buffer containing 2.5% dodecyl-β-maltoside, 20% glycerol, 25mM BisTris–HCl, 50mM 6-amino-caproic acid, pH 7.0, and 0.5% Coomassie Blue Serva G. After 20min of incubation at 20°C, the samples were subjected to 8% polyacrylamide gel and developed as described [5]. SDS-PAGE analysis in 5%–16% gradient gel was conducted according to a procedure described earlier [5].

## 3. Results

### 3.1. Lysenin-His adsorption at the air–water interface and insertion into the lipid bilayer

Lysenin is a toxin extruded into the coelomic fluid of *E. foetida* as a water-soluble protein, however, upon encountering a vertebrate cell it binds to the plasma membrane and evokes its permeation. This phenomenon indicates that lysenin is a surface-active molecule. To examine this property of lysenin-His, we investigated spontaneous adsorption of the protein at the air–water interface. The effects of the injection of 70nM lysenin-His into the water subphase exerted on the surface pressure at the air–water interface are shown in Fig. 1A. As can be seen, the protein injection to the aqueous phase leads to an increase of surface pressure, indicating that lysenin-His is surface-active and has an ability to adsorb at the air–water interface. During the initial phase of the experiment (the first 1500s) the changes in surface pressure

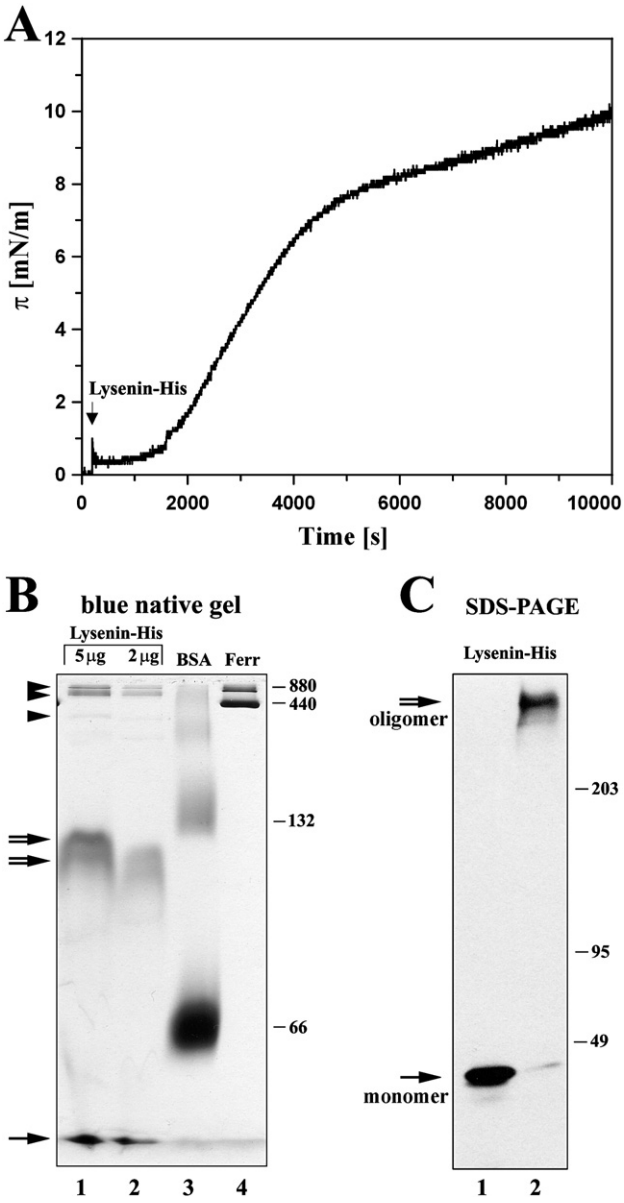


Fig. 1. (A) Time course of adsorption of lysenin-His at an argon–water interface. The deposition of lysenin at the interface was monitored by surface pressure changes in a Langmuir balance. An arrow indicates the injection of 20 μl of lysenin-His solution into 12 ml of buffer to a final concentration of 70 nM. (B) Blue native gel electrophoresis of 5 μg (lane 1) and 2 μg (lane 2) of lysenin-His in the absence of lipids. On the right, molecular weight of standards (lane 3 — BSA 66 kDa monomer and 132 kDa dimer; lane 4 — ferritin 440 kDa monomer and 880 kDa dimer) is indicated. On the left, arrowheads point to very large oligomers of lysenin-His, double arrows indicate trimers while monomer of lysenin-His is marked by arrow. (C) SDS-PAGE analysis of 2 μg of lysenin-His alone (lane 1) and after incubation with liposomes (lane 2) composed of sphingomyelin:phosphatidylcholine:cholesterol (3:7:3 molar ratio). Arrow indicates monomer and double arrow oligomer of lysenin-His. On the right, the position of standard proteins of known molecular weight is marked.

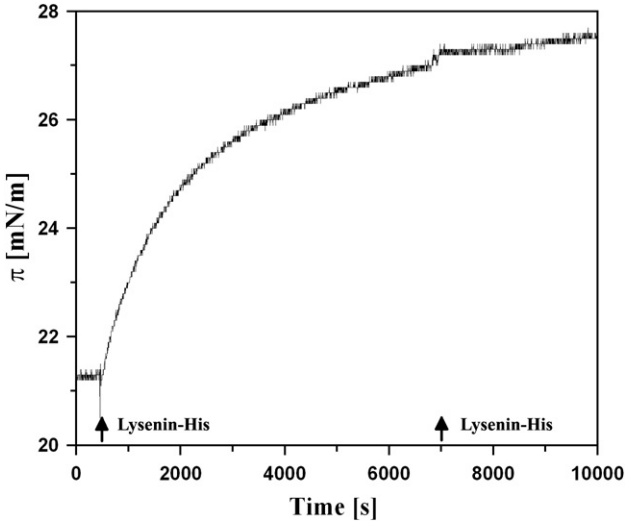


Fig. 2. Effect of lysenin-His on surface pressure of a lipid monolayer. Increase of surface pressure after injections (marked with arrows) of lysenin-His into the water subphase beneath the monomolecular layer formed with sphingomyelin: cholesterol (at the molar ratio 1:1) at the argon–water interface and maintained at the surface pressure of ~21.5 mN/m. Temperature 21 °C. After each injection the lysenin-His concentration in the subphase was increased by 70 nM.

are not significant. However, after the first 2000s, the surface pressure shows a pronounced increase of the rate of change (represented by the slope of the graph). After the first 5000s of the experiment adsorption of lysenin-His at the interface stabilizes at a low rate. Saturation of the process under these particular conditions (lysenin-His concentration, temperature etc.) was observed after 3h of the experiment (not shown). The steady state level of surface pressure under saturation conditions was close to 10mN/m. Such a profile of the surface pressure changes indicates that lysenin-His does not have strong surface-active properties, but rather cooperative adsorption of lysenin-His at the interface takes place with time. Such a cooperative character of changes suggested formation of molecular assemblies (oligomers) by lysenin-His in solution in the absence of lipids. The ability of self-association of lysenin-His in solution was confirmed using blue native gel electrophoresis (Fig. 1B). It was found that lysenin-His can exist in solution as both oligomers and monomer. The apparent molecular weight of the major doublet of the oligomers was 120kDa and 110kDa (Fig. 1B, double arrows). Lysenin-His formed also minute amounts of very large oligomers of about 800kDa, 620kDa and 410kDa (Fig. 1B, arrowheads) and remained partially as monomer (Fig. 1B, arrow). On the other hand, lysenin-His analyzed by SDS-PAGE at denaturing conditions migrated only as a single 41kDa band reflecting lysenin-His monomer (Fig. 1C, arrow) whereas lysenin-His bound to sphingomyelin-containing liposomes formed SDS-resistant hexamer of about 280kDa (Fig. 1C, double arrow).

Having established that lysenin-His is indeed a surface-active molecule, insertion of the protein into a lipid monolayer was studied. Fig. 2 presents the time course of surface pressure changes in the monomolecular lipid layer formed at the argon–water interface with a lipid mixture of sphingomyelin:cholesterol (1:1, by mol), followed by the injection of 70nM lysenin-His into the subphase. The composition of the monolayer ensued from the earlier findings that cholesterol increases the binding of lysenin-His to a sphingomyelin-containing membrane [4]. Immediately after the injection of the protein solution beneath the monolayer its lateral pressure begins to increase (Fig. 2). There is no lag phase, seen previously during adsorption of lysenin-His at the air–water interphase, which demonstrates direct binding of lysenin-His to the lipid layer (see Fig. 1A). The time dependency of the surface pressure changes of the lipid monolayer upon lysenin-His binding was highly reproducible and followed a saturation-type curve. Total surface pressure changes were close to 6mN/m, and a second injection of the protein beneath the monolayer did not change substantially the surface pressure, confirming that the kinetics represent a saturation-type dependency.

### 3.2. Secondary structure analysis of lysenin-His in soluble and membrane-bound form

The avid interaction of lysenin-His with the sphingomyelin-containing membrane prompted us to apply ATR-FTIR spectroscopy to study changes of the secondary structure of the protein accompanying the membrane insertion. Fig. 3 presents the FTIR absorption spectrum of lysenin-His collected with non-polarized light, deposited on a solid support, in the amide I frequency region, between 1700 and 1600cm$^{-1}$. Deconvolution of the amide I band with components that represent a combination of Gaussian and Lorentzian functions enabled the secondary structure of the protein to be determined [23]. All the spectral components are listed in Table 1. The sharp band centered at 1624cm$^{-1}$ is characteristic of aggregated strands. The area of this component accounts for 28% of the total area of the amide I band (Table 1). Two bands: the relatively weak one with the maximum at 1680cm$^{-1}$ and the strong one with the maximum at 1636cm$^{-1}$ can be assigned to β-sheet structures, with the 1680cm$^{-1}$ band being characteristic to anti-parallel β-sheet structure. Together, the high

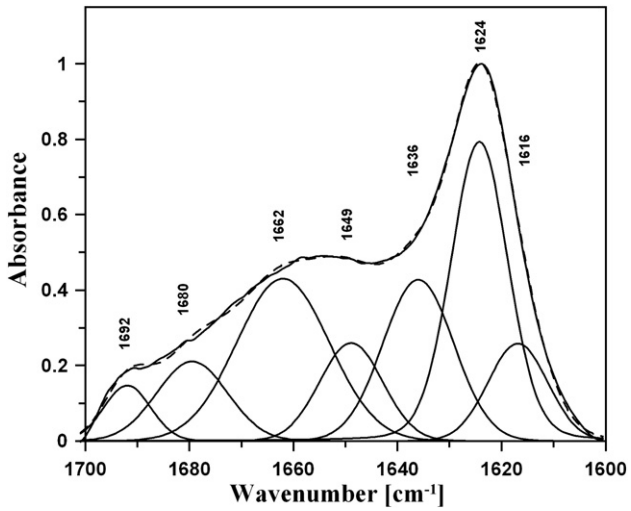


Fig. 3. ATR-FTIR absorption spectrum in amide I region of pure lysenin-His recorded with non-polarized light. Lysenin-His was deposited on a Ge support by evaporation from $D_2O$. The spectrum was normalized at the band maximum. The original spectrum (dashed line) is presented along with the fit (solid line) and deconvolution components (each being an even mixture of Lorentzian and Gaussian components). Assignment of the bands is presented in Table 1.

Table 1
Deconvolution of amide I band of lysenin

| Lysenin-His (pure) | | Lysenin-His in lipid bilayer | | Assignment |
|---|---|---|---|---|
| [$cm^{-1}$] | area [%] | [$cm^{-1}$] | area [%] | |
| 1691 | 3 | | | Aggregated form |
| 1680 | 9 | | | Anti-parallel β-sheet |
| 1662 | 23 | 1661 | 21 | Turns and loops |
| 1648 | 10 | 1649 | 13 | α-helix |
| 1636 | 18 | 1638 | 31 | β-sheet |
| 1624 | 28 | 1626 | 27 | Aggregated β-strands |
| 1616 | 9 | 1613 | 8 | Aggregated form |

Lysenin-His was deposited on the crystal by partial evaporation from $D_2O$. Alternatively, lysenin-His was bound to the lipid bilayer from the water subphase.

frequency and the low frequency components comprise 27% of all secondary structures of lysenin-His in the sample. Turns and loops (23%) give rise to the band with the maximum at 1662$cm^{-1}$ and the relatively small component with the maximum at 1648$cm^{-1}$ is characteristic of the α-helix structure (10%). The relatively small components that center at 1691$cm^{-1}$ and 1616$cm^{-1}$ were assigned to different kinds of aggregated structures.

To reveal the changes of the secondary structure of lysenin-His taking place during interaction with the membrane, we studied the ATR-FTIR absorption spectrum in the amide I region of lysenin-His bound to the lipid bilayer (sphingomyelin: cholesterol 1:1) deposited on the surface of the ATR crystal. Lysenin-His was bound to the membrane from the subphase, after the injection of the protein solution beneath the bilayer. Fig. 4 presents the IR absorption spectra of the membrane-bound lysenin-His, recorded with polarized light. In the case of axially-oriented samples deposited to ATR crystal, absorption

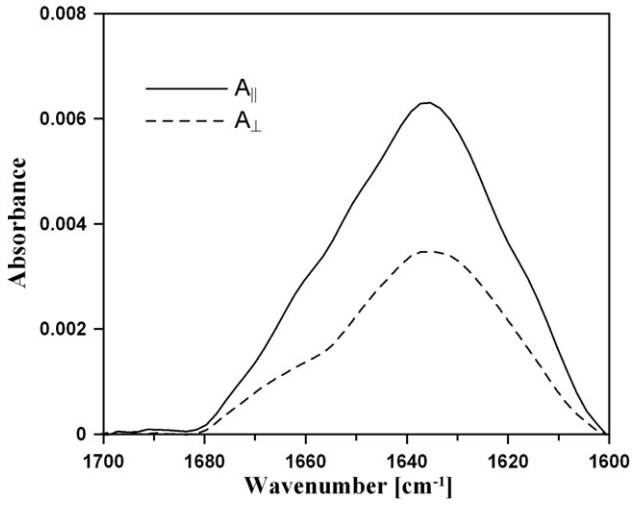


Fig. 4. Polarized ATR-FTIR absorption spectra in the amide I region of lipid bilayer-bound lysenin-His. A sphingomyelin:cholesterol bilayer was formed between the water subphase and the ATR crystal and maintained at the surface pressure of ~22 mN/m. Lysenin-His was injected beneath the bilayer at a final concentration in the subphase of 70 nM. The spectra were recorded with the electric vector of radiation polarized parallel ($A_{\parallel}$) or perpendicular ($A_{\perp}$) to the plane of incidence.

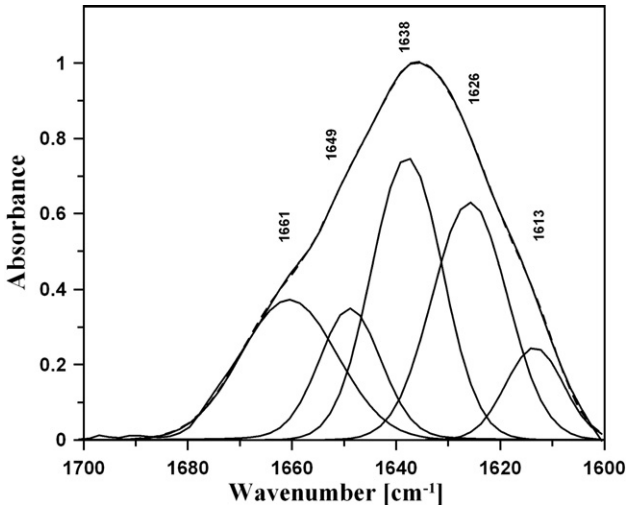


Fig. 5. ATR-FTIR "polarization-independent" spectrum in the amide I region of lipid bilayer-bound lysenin-His, obtained using the spectra recorded with polarized light (see Fig. 4). The spectrum was normalized at the band maximum. The original spectrum (dashed line) is presented along with the fit (solid line) and deconvolution components (each being an even mixture of Lorentzian and Gaussian components). Assignment of the bands is presented in Table 1.

spectrum has to be calculated as a linear combination of the absorption spectra recorded with electric vector of IR radiation polarized parallel and perpendicular with respect to the plane of incidence [22]. Owing to the fact that lysenin-His was incorporated to the oriented bilayer, absorption spectrum in the amide I region was calculated according to this rule. The spectrum was deconvoluted and analyzed in the same way as in the case of the pure protein deposited directly onto the crystal support (Fig. 5). The assignment of the component bands is as follows:1661$cm^{-1}$ turns and loops, 1649$cm^{-1}$ α-helix, 1638$cm^{-1}$ β-sheet, 1626$cm^{-1}$ aggregated β-strands, and 1613$cm^{-1}$ other aggregated structures (Table 1). A comparison of the secondary structure components of lysenin-His incorporated into the lipid bilayer and lysenin-His deposited on a solid support reveals differences that can be directly associated with the molecular mechanism of the binding of lysenin-His to the lipid membrane. As can be seen, the total content of α-helix and turns and loops remains almost unchanged. The total β-structure content, including β-sheets and aggregated β-strands, does not change either (55–58%). The intensity of the band centered at 1638$cm^{-1}$, characteristic of the β-sheet structure, increases in the spectrum of lysenin-His incorporated to the lipid bilayer as compared to the spectrum of pure lysenin-His deposited on the crystal support and remaining in the aggregated form. The similar effect of increase of β-sheet component in the presence of sphingomyelin was also detected with the use of circular dichroism by Ishitsuka and Kobayashi [8]. The 1638$cm^{-1}$ β-sheet band accounts for 31% of the total secondary structure forms and the comparison suggests that the relative increase of this fraction is associated with the disappearance of forms represented by bands located in the higher wavenumber region of the amide I band (1680$cm^{-1}$). The fraction of aggregated β-strands does not change significantly and accounts for 27% of total secondary structure forms. It could be

expected that the protein deposited on the solid support by means of partial evaporation (Fig. 3) remained in the aggregated form. Interestingly, also lysenin-His dissolved in the water phase and bound to the lipid membranes forms molecular aggregates (Fig. 5). It is highly probable that the spontaneous formation of those aggregated structures of lysenin-His in the sphingomyelin–cholesterol environment reflects oligomerization of the protein.

### 3.3. Orientation of membrane-bound lysenin-His

Linear dichroism measurements provide information on the orientation of individual segments of a protein bound to an oriented lipid bilayer. FTIR spectra of lysenin-His incorporated into the single two-component lipid bilayer composed of sphingomyelin and cholesterol, recorded with polarized light, are shown in Fig. 4. The protein was spontaneously incorporated into the membrane from the water subphase. The contribution of the individual secondary structure forms to the pronounced linear dichroism observed can be analyzed after deconvolution of the band recorded with different polarization of the incident radiation (Fig. 6). Mean orientation of the α-helix axis can be determined on the basis of linear dichroism measurements owing to the axially symmetric structure of a protein in this form [21]. In order to determine the dichroic ratio corresponding to the α-helix, the appropriate deconvolution components were integrated. Average orientation of the α-helix fragment of lysenin-His incorporated into the membrane was calculated according to Eq. (1) and the results of the determination are presented in Table 2. Interestingly,

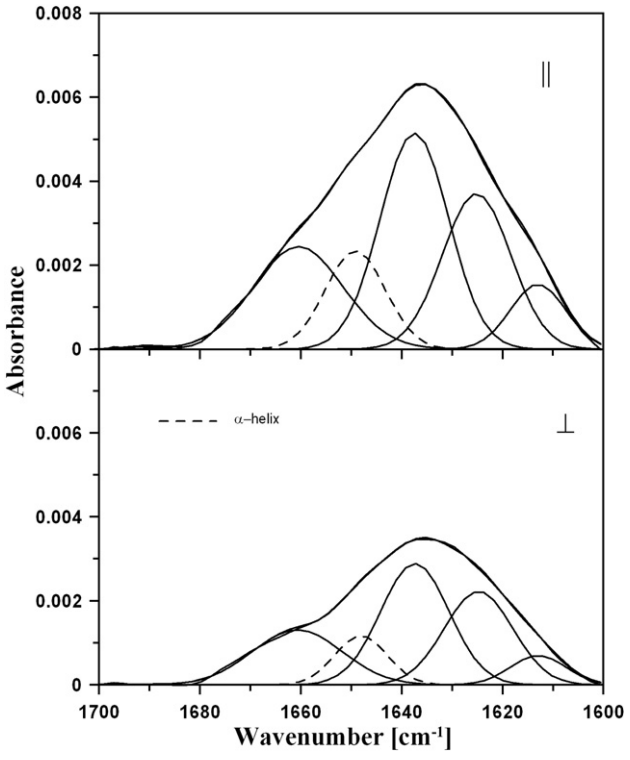


Fig. 6. Deconvolution analysis of the spectra presented in Fig. 5. Assignment of the bands as in Table 1. The dichroic ratio calculated for the band assigned to α-helix (1649 $cm^{-1}$), marked with dashed lines, is 2.25. Orientation of the protein segment calculated on the basis of linear dichroism spectra is given in Table 2.

Table 2
Average α-helix orientation in membrane-bound lysenin-His as determined by linear dichroism

| Band position [$cm^{-1}$] | Dichroic ratio $R$ [a] | Order parameter $S$ | $\alpha$ [deg] | $\theta$ [deg] |
|---|---|---|---|---|
| 1649 | 2.25 | 0.343 | 39 | 41 |

±SD: $S$ (±0.05), $\theta$ (±3°).
[a] Dichroic ratio was determined from the deconvolution component area following Eq. (1).

the average orientation of the α-helical segment of the protein, determined as 41°, is evidently lower than the magic angle. Such an orientation suggests that this protein segment may penetrate the lipid bilayer and be responsible for the docking of lysenin-His to the membrane.

## 4. Discussion

Upon binding to sphingomyelin-containing membranes, lysenin assemblies cation-selective channels and large membrane pores, thus leading to cell lysis [1,5,24,25]. To elucidate the mechanism of the lytic activity of lysenin, we analyzed the surface activity of the protein as well as changes of its secondary structure during interaction with sphingomyelin in membranes. We found that lysenin-His spontaneously adsorbed at the air–water interface as could be expected. After a long lag phase, when lysenin-His did not display any surface activity, a steep increase of the protein adsorption was observed (Fig. 1A). These data can suggest that while monomers of lysenin-His are not surface-active, in the course of experiment the protein monomers can slowly form assemblies in solution. In this scenario, the hydrophobicity of the lysenin-His assemblies would exceed that of monomers, driving adsorption of the protein complexes at the air–water interface. The ability of lysenin-His to self-associate in the absence of lipids was demonstrated by blue native gel electrophoresis. The analysis revealed that a fraction of lysenin-His existed in solution as trimer (120–110 kDa) accompanied by multioligomers and monomer. The discovery of oligomers of lysenin-His in solution defines a novel property of the protein. We should indicate, however, that lysenin used in our experiments was tagged with six histidine residues at the N-terminus and this modification could affect self-association of lysenin in solution. The role of the N-terminus of a protein in controlling oligomerization was demonstrated for Staphylococcal α-hemolysin. The N-terminus of this toxin prevented formation of premature oligomers of α-hemolysin in solution and, on the other hand, facilitated oligomerization of the protein after membrane binding [26].

A strong tendency of lysenin to form oligomeric structures has been demonstrated previously by SDS-PAGE, fluorescence, calorimetric and microscopic visualization studies [4,5,10]. However, in those studies, assembly of lysenin hexamers was strictly correlated with the interaction of the protein with sphingomyelin-containing membranes. It is of note that in contrast to hexamers of lysenin bound to sphingomyelin, the oligomers of lysenin-His in solution were sensitive to SDS treatment and upon SDS-PAGE the protein migrated as monomer of 41 kDa.

Measurements of surface pressure changes during interaction of lysenin-His with a sphingomyelin/cholesterol monolayer revealed an immediate insertion of the protein (Fig. 2). The lack of a lag phase found under these conditions, and the relatively high rate of initial surface pressure changes can be interpreted in terms of lipid-enhanced binding of the protein to the interfacial layer. A similar shape of the time course of surface pressure changes has been observed in the case of lysenin binding to monomolecular layers formed with sphingomyelin only [10]. Taken together, the data suggest that the lysenin–sphingomyelin interaction is faster and stronger than the lysenin–lysenin interaction in solution.

Binding of lysenin-His to sphingomyelin is accompanied by significant changes of the secondary structure of the protein, as we found using ATR-FTIR spectroscopy. The band at 1636 $cm^{-1}$, that can be assigned to parallel and anti-parallel β-sheet structures, increased from 18% to 31%. Simultaneously, the 1680 $cm^{-1}$ component (anti-parallel β-sheet) disappeared. As a result, the total β-structure content in the lysenin-His molecule remained almost unchanged upon membrane binding (Table 1). Interestingly, the determination of the secondary structure of lysenin-His based on the analysis of the amide I band revealed the presence of an α-helical segment (the 1648 $cm^{-1}$ component). The α-helix accounts for 10–13% of the protein secondary structure, both in soluble and membrane-bound lysenin-His. Despite the relatively low contribution of the α-helix to the entire lysenin-His secondary structure composition, the 41° angle of orientation of this protein segment, supports the assignment of the 1648 $cm^{-1}$ component as a distinct secondary structure of the protein. It is of note that the determination of the secondary structure of lysenin-His presented here, based on the analysis of the amide I band, is in relatively good agreement with our earlier results of secondary structure prediction using several approaches, as discussed by Shakor et al. [2]. It was predicted with high probability that one α-helix is located close to the C-terminus of lysenin (amino acids from 256 to 270), while amino acids 145–150 were found to have a low probability of forming another α-helix.

Linear dichroism analysis demonstrated that the α-helix (helices) is oriented at 41° angle to the normal to the membrane (Table 2). Such an angle of orientation indicates that the α-helix is located almost parallel to the mean direction of the membrane lipid chains [19]. Based on this data we tentatively identify the α-helix as a membrane-inserting one. Taking into account that the predicted α-helix encompasses 30 amino acid residues (10% out of total 297 amino acids) [2] and that the maximum change of surface pressure evoked by lysenin-His at the air–water interface was about 10 mN/m, the calculated value mN/m × residue equals 0.33. The value fits in the range of 0.1–1.0 mN/m × residue estimated by Sanchez-Magraner et al. [27] as typical for amphipatic structures found in several cytolysins. The presence of a small helical protein segment which can be potentially directly anchored within the membrane seems to be particularly interesting in terms of the possible mechanisms of interaction of lysenin with biomembranes. It indicates that lysenin belongs to a group of toxins, including e.g., bacterial colicins and actinoporins of sea anemones which exert the lytic activity by insertion of preexisting α-helices into the membrane [28–30]. The C-terminal 30 amino acids which directly follow the putative α-helix and are predicted with high probability to be arranged into three β-strands [2] are also important for bioactivity of the protein. After deletion of the last 15 amino acids from the C-terminus, sphingomyelin binding of lysenin was abrogated [6].

At present, we can hypothesize that lysenin binds to the membrane by exposed aromatic residues, including tryptophans crucial for sphingomyelin recognition [3]. Studies of Kobayashi's group [4] confirmed that upon binding of lysenin to sphingomyelin in membranes tryptophan residues become embedded into less polar environment. In the view of our findings that lysenin can exist in solution as premature oligomers (mainly trimers, Fig. 1B) and that lysenin trimer was identified as a functional unit of the protein bound to sphingomyelin [5] we cannot rule out the possibility that preformed trimers of lysenin interact with sphingomyelin in the membrane. Upon membrane binding, lysenin further oligomerizes to form hexamers. A similar mechanism of action has been proposed for adenylate cyclase toxin of *Bordetella pertussis* [31]. However, the steep slope of insertion of lysenin-His into the sphingomyelin:cholesterol monolayer (compare Figs. 1A and 2) suggests that the rate of binding of lysenin monomers to sphingomyelin exceeds that of lysenin oligomerization in solution. The exposure of hydrophobic residues of lysenin and/or oligomerization of the protein during sphingomyelin binding might be responsible for the reorganization of β-structures of lysenin-His found by ATR-FTIR (Figs. 3 and 5). The α-helices of the lysenin oligomers penetrate the membrane and form water-permeable pores owing to their amphipatic character. The coupling between oligomerization and membrane permeation is common to numerous cytotoxins [26,32,33]. In general terms, the mechanism of lysenin action can resemble that of equinatoxin, a pore-forming toxin from sea anemone *Actinia equina*. In the current model of pore formation, equinatoxin β-sandwich structure stabilizes the interaction of the protein with sphingomyelin in the membrane allowing protein oligomerization and exposure of an α-helix which inserts into the membrane and participates in pore assembly [29,33,34].

## Acknowledgements

We thank Dr. Edward Czuryło (Nencki Institue of Experimental Biology, Warsaw, Poland) for providing some samples of recombinant lysenin-His. This work was supported by Grant no. PBZ/MEiN/01/2006/44 from the Polish Ministry of Higher Education and Science to M. Hereć and by Grant no. 2P04C 141 29 from the Polish Ministry of Higher Education and Science to A. Sobota.

## References

[1] A. Yamaji, Y. Sekizawa, K. Emoto, H. Sakuraba, K. Inoue, H. Kobayashi, M. Umeda, Lysenin, a novel sphingomyelin-specific binding protein, J. Biol. Chem. 273 (1998) 5300–5306.

[2] A.B. Shakor, E.A. Czurylo, A. Sobota, Lysenin, a unique sphingomyelin-binding protein, FEBS Lett. 542 (2003) 1–6.

[3] E. Kiyokawa, A. Makino, K. Ishii, N. Otsuka, A. Yamaji-Hasegawa, T. Kobayashi, Recognition of sphingomyelin by lysenin and lysenin-related proteins, Biochemistry 43 (2004) 9766–9773.
[4] A. Yamaji-Hasegawa, A. Makino, T. Baba, Y. Senoh, H. Kimura-Suda, S.B. Sato, N. Terada, S. Ohno, E. Kiyokawa, M. Umeda, T. Kobayashi, Oligomerization and pore formation of a sphingomyelin-specific toxin, lysenin, J. Biol. Chem. 278 (2003) 22762–22770.
[5] K. Kwiatkowska, R. Hordejuk, P. Szymczyk, M. Kulma, A.B. Abdel-Shakor, A. Pluciennicza k, K. Dolowy, A. Szewczyk, A. Sobota, Lysenin-His, a sphingomyelin-recognizing toxin, requires tryptophan 20 for cation-selective channel assembly but not for membrane binding, Mol. Membr. Biol. 24 (2007) 121–134.
[6] E. Kiyokawa, T. Baba, N. Otsuka, A. Makino, S. Ohno, T. Kobayashi, Spatial and functional heterogeneity of sphingolipid-rich membrane domains, J. Biol. Chem. 280 (2005) 24072–24084.
[7] T. Ide, T. Aoki, Y. Takeuchi, T. Yanagida, Lysenin forms a voltage-dependent channel in artificial lipid bilayer membranes, Biochem. Biophys. Res. Commun. 346 (2006) 288–292.
[8] R. Ishitsuka, T. Kobayashi, Cholesterol and lipid/protein ratio control the oligomerization of a sphingomyelin-specific toxin, lysenin, Biochemistry 46 (2007) 1495–1502.
[9] R. Ishitsuka, T. Kobayashi, Lysenin: a new tool for investigating membrane lipid organization, Anat. Sci. Int. 79 (2004) 184–190.
[10] R. Ishitsuka, A. Yamaji-Hasegawa, A. Makino, Y. Hirabayashi, T. Kobayashi, A lipid-specific toxin reveals heterogeneity of sphingomyelin-containing membranes, Biophys. J. 86 (2004) 296–307.
[11] K. Simons, D. Toomre, Lipid rafts and signal transduction, Nat. Rev., Mol. Cell Biol. 1 (2000) 31–39.
[12] D. Holowka, J.A. Gosse, A.T. Hammond, X. Han, P. Sengupta, N.L. Smith, A. Wagenknecht-Wiesner, M. Wu, R.M. Young, B. Baird, Lipid segregation and IgE receptor signaling: a decade of progress, Biochim. Biophys. Acta 1746 (2005) 252–259.
[13] V. Michel, M. Bakovic, Lipid rafts in health and disease, Biol. Cell 99 (2007) 129–140.
[14] Y. Sekizawa, T. Kubo, H. Kobayashi, T. Nakajima, S. Natori, Molecular cloning of cDNA for lysenin, a novel protein in the earthworm *Eisenia foetida* that causes contraction of rat vascular smooth muscle, Gene 191 (1997) 97–102.
[15] L. Silvestro, P.H. Axelsen, Membrane-induced folding of cecropin A, Biophys. J. 79 (2000) 1465–1477.
[16] S.A. Tatulian, L.R. Jones, L.G. Reddy, D.L. Stokes, L.K. Tamm, Secondary structure and orientation of phospholamban reconstituted in supported bilayers from polarized attenuated total reflection FTIR spectroscopy, Biochemistry 34 (1995) 4448–4456.
[17] H. Binder, Infrared dichroism investigations on the acyl chain ordering in lamellar structures. III. Characterization of the chain tilt and biaxiality in the solid phases of dipalmitoilphosphatidylcholine as a function of temperature and hydration using molecular order parameters, Vibr. Spectrosc. 21 (1999) 151–163.
[18] G. Menestrina, Use of Fourier-transformed infrared spectroscopy (FTIR) for secondary structure determination of staphylococcal pore-forming toxins, in: O. Holst (Ed.), Bacterial Toxins, Methods and Protocols, Humana Press, Totowa, New Jersey, 2000, pp. 115–132.
[19] M. Gagos, J. Gabrielska, M. Dalla Serra, W.I. Gruszecki, Binding of antibiotic amphotericin B to lipid membranes: monomolecular layer technique and linear dichroism-FTIR studies, Mol. Membr. Biol. 22 (2005) 433–442.
[20] H. Binder, T. Gutberlet, A. Anikin, Biaxial ordering of terminal diene groups in lipid membranes: an infrared linear dichroism, J. Mol. Struct. 510 (1999) 113–129.
[21] L.K. Tamm, S.A. Tatulian, Infrared spectroscopy of proteins and peptides in lipid bilayers, Q. Rev. Biophys. 30 (1997) 365–429.
[22] D. Marsh, Quantification of secondary structure in ATR infrared spectroscopy, Biophys. J. 77 (1999) 2630–2637.
[23] S.A. Tatulian, L.K. Tamm, Secondary structure, orientation, oligomerization, and lipid interactions of the transmembrane domain of influenza hemagglutinin, Biochemistry 39 (2000) 496–507.
[24] S. Lange, F. Nussler, E. Kauschke, G. Lutsch, E.L. Cooper, Herrmann, Interaction of earthworm hemolysin with lipid membranes requires sphingolipids, J. Biol. Chem. 272 (1997) 20884–20892.
[25] E.L. Cooper, E. Kauschke, A. Cossarizza, Digging for innate immunity since Darwin and Metchnikoff, BioEssays 24 (2002) 319–333.
[26] L. Jayasinghe, G. Miles, H. Bayley, Role of the amino latch of staphylococcal α-hemolysin in pore formation: a co-operative interaction between the N terminus and position 217, J. Biol. Chem. 281 (2006) 2195–2204.
[27] L. Sanchez-Magraner, A.L. Cortajarena, F.M. Goni, H. Ostolaza, Membrane insertion of *Escherichia coli* α-hemolysin is independent from membrane lysis, J. Biol. Chem. 281 (2006) 5461–5567.
[28] C. Lesieur, B. Vecsey-Semjen, L. Abrami, M. Fivaz, F. Gisou van der Goot, Membrane insertion: the strategies of toxins (review), Mol. Membr. Biol. 14 (1997) 45–64.
[29] G. Anderluh, M. Dalla Serra, G. Viero, G. Guella, P. Macek, G. Menestrina, Pore formation by equinatoxin II, a eukaryotic protein toxin, occurs by induction of nonlamellar lipid structures, J. Biol. Chem. 278 (2003) 45216–45223.
[30] A. Drechsler, C. Potrich, J.K. Sabo, M. Frisanco, G. Guella, M. Dalla Serra, G. Anderluh, F. Separovic, R.S. Norton, Structure and activity of the N-terminal region of the eukaryotic cytolysin equinatoxin II, Biochemistry 45 (2006) 1818–1828.
[31] S.J. Lee, M.C. Gray, K. Zu, E.L. Hewlett, Oligomeric behavior of *Bordetella pertussis* adenylate cyclase toxin in solution, Arch. Biochem. Biophys. 438 (2005) 80–87.
[32] M. Palmer, R. Harris, C. Freytag, M. Kehoe, J. Tranum-Jensen, S. Bhakdi, Assembly mechanism of the oligomeric streptolysin O pore: the early membrane lesion is lined by a free edge of the lipid membrane and is extended gradually during oligomerization, EMBO J. 17 (1998) 1598–1605.
[33] K. Kristan, Z. Podlesek, V. Hojnik, I. Gutierrez-Aguirre, G. Guncar, D. Turk, J.M. Gonzalez-Manas, J.H. Lakey, P. Macek, G. Anderluh, Pore formation by equinatoxin, a eukaryotic pore-forming toxin, requires a flexible N-terminal region and a stable β-sandwich, J. Biol. Chem. 279 (2004) 46509–46517.
[34] I. Gutierrez-Aguirre, A. Barlic, Z. Podlesek, P. Macek, G. Anderluh, J.M. Gonzalez-Manas, Membrane insertion of the N-terminal α-helix of equinatoxin II, a sea anemone cytolytic toxin, Biochem. J. 384 (2004) 421–428.